



**HAL**  
open science

## Self-Photopolymerization of Poly(disulfide) Oligomers

Abraham Chemtob, Noémi Feillée, Cyril Vaultot, Christian Ley, Didier Le Nouen

► **To cite this version:**

Abraham Chemtob, Noémi Feillée, Cyril Vaultot, Christian Ley, Didier Le Nouen. Self-Photopolymerization of Poly(disulfide) Oligomers. ACS Omega, 2019, 4 (3), pp.5722-5730. 10.1021/acsomega.9b00021 . hal-02434784

**HAL Id: hal-02434784**

**<https://hal.science/hal-02434784>**

Submitted on 10 Jan 2020

**HAL** is a multi-disciplinary open access archive for the deposit and dissemination of scientific research documents, whether they are published or not. The documents may come from teaching and research institutions in France or abroad, or from public or private research centers.

L'archive ouverte pluridisciplinaire **HAL**, est destinée au dépôt et à la diffusion de documents scientifiques de niveau recherche, publiés ou non, émanant des établissements d'enseignement et de recherche français ou étrangers, des laboratoires publics ou privés.

# Self-Photopolymerization of Poly(disulfide) Oligomers

Abraham Chemtob,<sup>\*,†,‡,§</sup> Noémi Feillé,<sup>‡,§</sup> Cyril Vaultot,<sup>†,‡</sup> Christian Ley,<sup>‡,§</sup> and Didier Le Nouen<sup>||</sup>

<sup>†</sup>Université de Haute-Alsace, CNRS, IS2M UMR7361, F-68100 Mulhouse, France

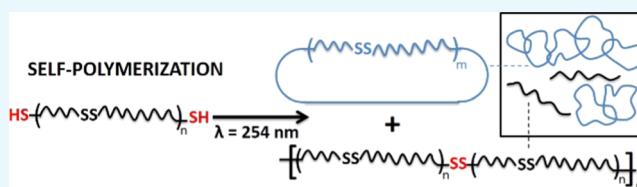
<sup>‡</sup>Université de Strasbourg, Strasbourg, France

<sup>§</sup>Université de Haute-Alsace, LPIM EA4567, F-68100 Mulhouse, France

<sup>||</sup>Université de Haute-Alsace, Université de Strasbourg, CNRS, LIMA UMR7042, F-68100 Mulhouse, France

## Supporting Information

**ABSTRACT:** Base catalyst and oxidant are usually necessary to promote the polymerization of poly(disulfide) oligomers through oxidative coupling of the terminal SH groups into S–S bonds. In this study, we prove that self-polymerization of bifunctional (disulfide) oligomer films can take place in a matter of minutes under UVC irradiation (254 nm, 10.5 mW cm<sup>-2</sup>). The resulting insoluble polymer is characterized using solid-state NMR, <sup>1</sup>H T<sup>2</sup> NMR relaxation measurements, thermal analysis, and Fourier-transform infrared spectroscopy and proves to have similar composition as a model poly(disulfide) prepared under oxidative conditions, but distinct physical properties. These differences are explained by a change in polymer architecture due to a higher ratio of cyclization relative to linear polymerization. Homolytic photocleavage of internal S–S bonds creates thiyl groups close to each other, driving an increased kinetic feasibility for the cyclization reaction by radical coupling. The subsequent formation of mechanically interlocked macrocycles (polycatenane network) is proposed to account for film properties analogous to those of a cross-linked polymer.



## I. INTRODUCTION

Most of the radiation-induced polymerizations described in the literature require the presence of a photoinitiator.<sup>1</sup> In a chain photopolymerization for instance, the photoinitiator's decomposition results in radical, anionic, or cationic reactive centers. Once produced, these species can add many monomer units to yield a high-molecular-weight polymer. However, some photopolymerizations are also possible without the addition of an external initiator, providing benefits in terms of polymer properties and reliability, including resistance to aging or exposure to weather conditions, and reduced content of leachable compounds in the plastics materials. The main developments in this field are based on ionizing radiations, produced by beams of particles or photons whose energy is sufficient to produce radicals and/or ionized species through direct excitation of monomer molecules: electron beams mainly, but also to a less extent hard X-rays and  $\gamma$  and  $\beta$  radiations.<sup>2,3</sup> By contrast, examples relying on less energetic radiations in the UV range are much more limited. Most of them are based on a radical-type polymerization self-initiated under UVC irradiation (100–280 nm), which can be provided by conventional UV lamps less costly to operate and maintain than electron beam processing. In this regard, Bowman et al. demonstrated that thiol-ene photopolymerization could be achieved without the addition of a radical photoinitiator. Initiating thiyl radicals were photogenerated through homolytic cleavage of thiol groups at 254 nm; higher wavelengths (365 nm) were even permitted with more labile thiols.<sup>4,5</sup> Another strategy consisted of the UVC irradiation of specific electron-donor/-acceptor monomers

bearing a maleimide chromophore group.<sup>6</sup> However, the main developments concerned chemically modified acrylate monomers such as vinyl or brominated acrylates.<sup>7</sup> In addition, self-initiation of conventional alkyl acrylates proved possible under an excimer lamp (222 or 172 nm)<sup>8</sup> or even under a conventional unfiltered medium-pressure Hg lamp (250–800 nm).<sup>9</sup> Despite these developments, it is still of high interest to extend the range of self-photopolymerizable structures.

In this report, we show that linear poly(disulfide) (PdS) oligomer films (HS-(R-SS)<sub>n</sub>-SH) can form cross-linked insoluble polymers within minutes when irradiated alone at 254 nm. Although less common than polyester or polyurethane resins, liquid low molecular weight PdS containing internal disulfide bonds are commercial and commonly referred by their trade name Thiokol or Thioplast. They are extensively used as technical joints for aerospace, construction, and double glazing—some niche applications where their high barrier properties and solvent resistance are requested.<sup>10,11</sup> The advantage of this solventless cross-linking method would be to form PdS coatings with high energy efficiency and no additives. As shown in Figure 1, a conventional polymerization (path 1) includes, on the contrary, a base catalyst and an oxidant. A bifunctional PdS oligomer is then chain extended (or cross-linked with higher functionality oligomers) through oxidative coupling of the terminal SH groups into S–S bonds. In contrast,

Received: January 3, 2019

Accepted: March 13, 2019

Published: March 22, 2019

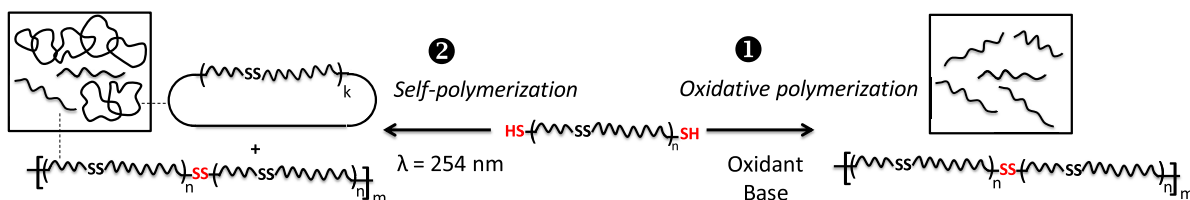


**Figure 1.** Path 1 is a chain extension of PdS resins through a conventional oxidative polymerization. Path 2 converts linear PdS oligomers into a polycatenane network by bulk self-photopolymerization under UVC irradiation.

our process proceeds without catalyst, oxidant, and solvent, suggesting a different reaction mechanism. As depicted in path 2 of Figure 1, we hypothesize UVC radiation to have a twofold effect: first, it produces thiyl radicals through homolytic cleavage, and subsequent reaction of these functional end groups with each other causes chain extension. Second, it may trigger the rearrangement of covalently reversible internal S–S bonds converting originally linear PdS chains into macrocycles. Because of solvent-free conditions, mechanical entanglement of cycles takes place, resulting in cross-linking. As a result, the network that forms would consist of linear chains together with interlocked cycles termed as a polycatenane network.<sup>12</sup>

Molecular catenanes are well-established structures, highly sought after to form prototypes of molecular machines inspired by nature (DNA, polypeptides).<sup>13</sup> The formation of polycatenane disulfide networks has already been reported in the literature, although their precise identification remains very difficult to prove.<sup>14</sup> Conducted by Endo et al., the synthesis conditions used initiator-less bulk polymerization of 1,2-dithiane above its melting point.<sup>15,16</sup> In addition, the photodynamic properties of disulfide-based molecules and polymers under UVC excitation have long been known. Bookwalter et al. showed in 1995 that the dominant pathway of dissociation of aliphatic disulfide molecules following excitation at 248 nm is the cleavage of the S–S bond.<sup>17</sup> This cleavage of the S–S bond leads to the formation of thiyl radicals capable of reacting in different chemical processes. Another reported reaction is disulfide–disulfide metathesis. Otsuka et al. reported in 2009 the synthesis of a polymer with dynamic properties through this S–S exchange under UV irradiation (254 nm).<sup>18</sup> However, it has only been recently that these dynamic properties have been exploited to create a self-healing polymer<sup>19–22</sup> or to degrade cross-linked materials<sup>23</sup> but never before to induce cross-linking.

Herein, we begin with a liquid film based on a difunctional PdS resin ( $\text{PdS}_{\text{SH1}}$ ,  $\text{HS}-(\text{R}-\text{SS})_n-\text{SH}$  with  $\text{R} = \text{CH}_2\text{CH}_2\text{OCH}_2\text{OCH}_2\text{CH}_2$ ,  $1100 \text{ g mol}^{-1}$ ). Self-photopolymerization (path d 2) was induced by irradiation with a low-pressure Hg arc (254 nm). To support the above-mentioned polymerization mechanism, a comparison was made with a model oxidative polymerization (path 1) using atmospheric oxygen as the oxidant<sup>24</sup> and 1,5,7-triazabicyclo[4.4.0]dec-5-ene (TBD), a bicyclic guanidine, as the base catalyst. In an effort to make the comparison more meaningful, this latter reaction was photochemically triggered using a xanthone propionic acid-protected TBD as the photobase generator (PBG)<sup>25,26</sup> and a 365 nm UV LED to avoid PdS absorption. To gain a better understanding of the self-photopolymerization mechanism, chemical and physical properties between the two polymers were investigated using a range of characterization techniques, including solid-state NMR,  $^1\text{H}$  T<sup>2</sup> NMR relaxation measurements, thermal analysis, and Fourier-transform infrared (FTIR) spectroscopy.

## II. RESULTS AND DISCUSSION

**II.1. Qualitative Experiments of PdS Self-Photopolymerization.** To assess the self-initiation ability of bifunctional PdS oligomers under UVC, scouting experiments were performed using two different UV sources: a low-pressure Hg arc (254 nm) and a medium-pressure Hg arc (200–500 nm). Their emission spectra together with the absorption spectrum of  $\text{PdS}_{\text{SH1}}$ , used as a model PdS resin, are shown in Figure 2.

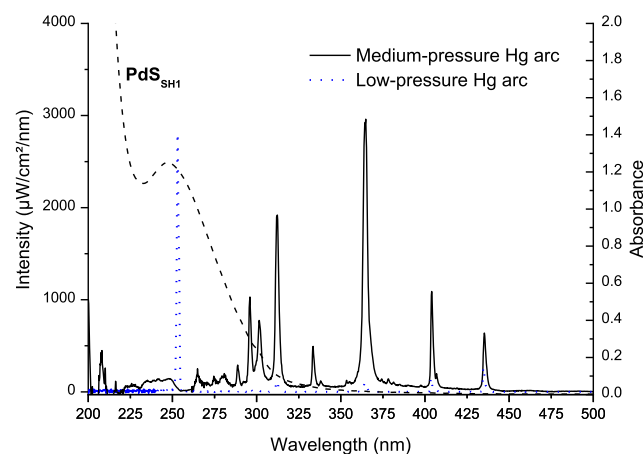
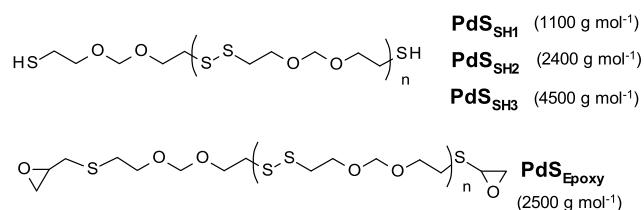


**Figure 2.** Absorption spectra of liquid poly(disulfide)  $\text{PdS}_{\text{SH1}}$  in acetonitrile ( $3.4 \times 10^{-4} \text{ M}$ ) and emission spectra of the two UV lamps used to induce its self-polymerization: medium-pressure Hg-Xe arc with a reflector at 254 nm and a low-pressure Hg arc.

$\text{PdS}_{\text{SH1}}$  displays a wide absorption band between 230 and 320 nm, which is assigned to the combined absorption of disulfide and thiol bonds.<sup>27,28</sup> Attributed mainly to the  $\pi-\sigma^*$  molecular orbital transition of SS bridges, the maximum at 248 nm is very close to the emission band of the low-pressure Hg arc at 254 nm. At this excitation wavelength, several studies demonstrated the possibility of S–S bonds' homolytic cleavage/metathesis<sup>28,29</sup> as well as H abstraction of S–H bonds.<sup>5</sup>

Using the polychromatic medium-pressure Hg arc (200–500 nm),  $\text{PdS}_{\text{SH1}}$  yields a solid film after 5 min irradiation. The film turned out to be fully insoluble in all tested organic solvents (chloroform, toluene, and THF). Substituting  $\text{PdS}_{\text{SH1}}$  with thiol oligomers of higher molar masses ( $\text{PdS}_{\text{SH2}}$ :  $2400 \text{ g mol}^{-1}$ ;  $\text{PdS}_{\text{SH3}}$ :  $4500 \text{ g mol}^{-1}$ ; Scheme 1) or with a  $\text{PdS}_{\text{epoxy}}$  exhibiting epoxy terminal groups ( $2600 \text{ g mol}^{-1}$ ) led to the same outcome. Interestingly, irradiation of  $\text{PdS}_{\text{SH-1}}$  under inert atmosphere also allowed solidification, which occurred at the same rate. However, when the emission of the medium-pressure arc was filtered to cut all wavelengths below 330 nm (borosilicate glass filter), the film remained in a liquid state. Conversely, a quasi-monochromatic low-pressure Hg arc ( $\lambda = 254 \text{ nm}$ ) led to dry films after 8 min irradiation. This set of results highlights the prevalent role of disulfide bridges in the photochemical

## Scheme 1. Structure of PdS Oligomers



mechanism. Indeed, dry films were obtained only when S–S bonds were excited. The ability of  $\text{PdS}_{\text{epoxy}}$  to produce a solid film reveals that terminal SH groups are not required to obtain a solid/cross-linked structure. Moreover, a solidification is observed for a range of PdS molar masses and without the need for atmospheric oxygen. Therefore, the self-photopolymerization process of PdS oligomers is flexible and unlikely to take place via a photo-oxidation mechanism.

**II.II. Comparison between Oxidative Photopolymerization and Self-Photopolymerizations of PdS. II.II.I. Solid-State NMR.** Starting from the oligomer  $\text{PdS}_{\text{SH1}}$ , the self-photopolymerized film  $\text{poly}(\text{PdS}_{\text{SH1}})$  obtained by irradiation with a low-pressure Hg lamp (254 nm) was analyzed by <sup>1</sup>H MAS NMR spectroscopy. Its structure was compared with  $\text{poly}(\text{PdS}_{\text{SH1}}/\text{PBG})$  obtained by oxidative photopolymerization (365 nm, with PBG). In this latter case, a mostly linear structure is expected because reaction proceeds essentially by chain extension through oxidative coupling between terminal SH groups (path 1, Figure 1). Because both films were insoluble, solid-state NMR seemed a relevant characterization technique. Figure 3 compares the <sup>1</sup>H MAS spectra of the two as-irradiated

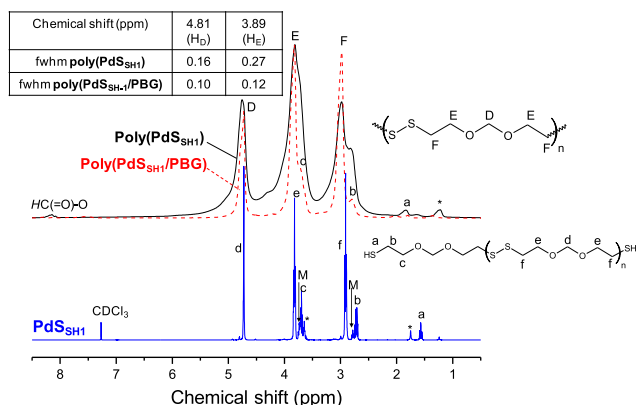


**Figure 3.** A. <sup>1</sup>H MAS NMR spectra of  $\text{poly}(\text{PdS}_{\text{SH1}})$  (—) and  $\text{poly}(\text{PdS}_{\text{SH1}}/\text{PBG})$  (- - -). At the bottom, the <sup>1</sup>H liquid NMR spectrum of the  $\text{PdS}_{\text{SH1}}$  resin in  $\text{CDCl}_3$ . M, monosulfide derivatives; \*, impurities. The inset gives the full width at half-maximum (fwhm) of the resonances corresponding to protons H<sub>D</sub> and H<sub>E</sub>.

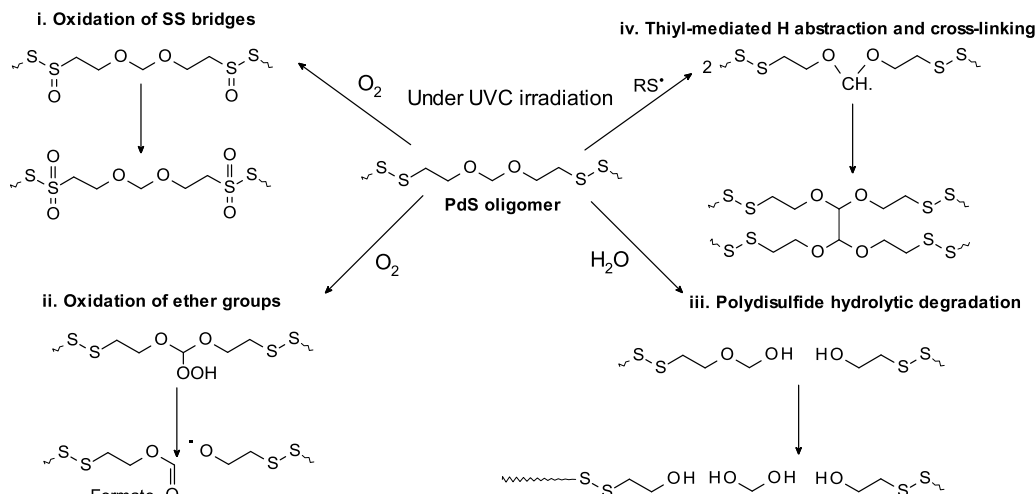
polymers as well as the spectrum of the original  $\text{PdS}_{\text{SH1}}$  oligomer. The spectra of the two photopolymers showed strong similarities, suggesting that the chain backbone was preserved in  $\text{poly}(\text{PdS}_{\text{SH1}})$ . However, two differences can be noticed. First, a significant signal broadening for  $\text{poly}(\text{PdS}_{\text{SH1}})$  compared to  $\text{poly}(\text{PdS}_{\text{SH1}}/\text{PBG})$  was observed, as exemplified by the increase of the resonance line widths of the methylene protons H<sub>D</sub> and H<sub>E</sub> (see inserted table in Figure 3). This can be understood on the basis of a more rigid structure formed under UVC irradiation. Second, the self-polymerized sample showed a weak thiol proton signal at 1.84 ppm (H<sub>a</sub>). A thiol conversion of

90% was calculated versus 98% with  $\text{poly}(\text{PdS}_{\text{SH1}}/\text{PBG})$ . In addition, the resonance associated with thiol protons in  $\text{poly}(\text{PdS}_{\text{SH1}})$  was shifted toward higher chemical displacements (+0.27 ppm) compared with  $\text{PdS}_{\text{SH1}}$ . This displacement may be due to a change in the environment of the -SH protons, between a viscous resin and a “polymerized” material. Note that similar line broadening and thiol conversions were obtained from the <sup>13</sup>C MAS + DEC NMR spectra available in the Supporting Information (Figure S1 of the Supporting Information). Consequently, these first results appear to minimize the occurrence of a UVC-induced chemical modification of ether or disulfide units constituting the polymer backbone of  $\text{PdS}_{\text{SH1}}$ . Nonetheless, all the possible degradation reactions are described in Scheme 2 and their occurrence examined on a case-to-case basis.

On the basis of studies dealing with PdS degradation, four possible side reactions may take place: oxidation of disulfide (i) and ether groups (ii), polydisulfide hydrolytic degradation (iii), and thiol-mediated hydrogen abstraction leading to cross-linking (iv).

- Oxidation of S–S bonds causes the formation of sulfonic, sulfinic, or sulfoxide groups. However, we did not observe the expected chemical shift of the -CH- groups moving downfield due to the effect of an adjacent S=O group in the <sup>1</sup>H (2.8–3.30 ppm) and <sup>13</sup>C spectra (46–60 ppm; see Figure S1 in SI),<sup>30</sup> thus supporting the absence of disulfide bridge oxidation.<sup>31</sup>
- Oxidation of poly(ethylene oxide) or poly(methylene oxide) is known to form the characteristic formate groups.<sup>32</sup> C–H adjacent to O atom forms a hydroperoxide, followed by scission to yield a formate. In favor of this hypothesis, the <sup>1</sup>H NMR spectrum of  $\text{poly}(\text{PdS}_{\text{SH1}})$  displayed a low intense peak around 8.15 ppm assigned to HC(=O)-O. However, this resonance accounts for only 0.5% of the total number of protons, evidencing the minor character of this side reaction.
- Previous studies emphasized the role of the hydrolytic path in the degradation of PdS oligomers leading to the formation of hydroxyl-containing compounds.<sup>33</sup> Support for this reaction was provided by the <sup>13</sup>C spectrum, which yielded a characteristic resonance at 61.3 ppm (see Figure S1 in SI). Again, the low intensity of the signal downplays the role attributable to hydrolyzed species.
- Finally, the last cross-linking route derives from the assumption of Mahon.<sup>33</sup> Homolytic cleavage of thiol yields a thiyl radical, which, in turn, reacts via hydrogen abstraction with methylene from the chain backbone, likely the CH<sub>2</sub> surrounded by two oxygen atoms exhibiting the weakest C–H bonds. The resultant carbon-centered radicals from different chains can recombine to form cross-links. However, such a route is unlikely because of the absence of tertiary carbon in the <sup>13</sup>C spectrum (expected at 100 ppm).<sup>34</sup> Additional proof was also provided by the <sup>13</sup>C DEPT 135° analysis of the  $\text{poly}(\text{PdS}_{\text{SH1}})$  (Figure S2 in SI).

**II.II.II. Relaxation Times by Low Field NMR.** The measurement of relaxation times by low field NMR makes it possible to differentiate the variations in segment mobility in a polymer and especially between linear or cross-linked systems.<sup>35</sup> The sensitivity of relaxation time measurement to chemical heterogeneities at the molecular level is due to the local origin of relaxation, dominated by the environment near the proton. In

Scheme 2. Four Types of Photoinduced Degradation Reactions Involving PdS Oligomers<sup>a</sup>

<sup>a</sup>Oxidation of disulfide bridges (i), oxidation (ii) or hydrolysis (iii) of the polyether chain, and self-cross-linking between alkyl radicals (iv).

particular, the  $T_2$  transverse relaxation time is directly related to the mobility of the segment on which the proton is located. To measure transverse relaxation time, we used a conventional CPMG sequence. Figure 4 shows the decrease in magnetization

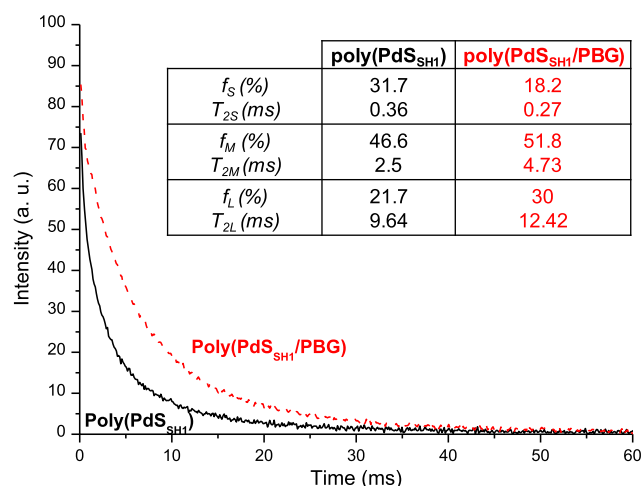


**Figure 4.** Decay of transverse magnetization of poly(PdS<sub>SH1</sub>) (—) and poly(PdS<sub>SH1</sub>/PBG) (---). The inserted table gives the relaxation times  $T_{2i}$  for the three types of protons associated with short time ( $T_{2S}$ ), intermediate time ( $T_{2M}$ ), and long time ( $T_{2L}$ ) with the corresponding volume fractions  $f_i$ .

over time for poly(PdS<sub>SH1</sub>) and poly(PdS<sub>SH1</sub>/PBG). In both cases, the measured magnetization  $M(t)$  of the material shows two different profiles, which can be represented by a function with three components, revealing a heterogeneity in terms of mobility in the two polymers. In simplified terms, the measured total magnetization relaxation  $M(t)$  is a weighted sum of the relaxations of the different submolecules:

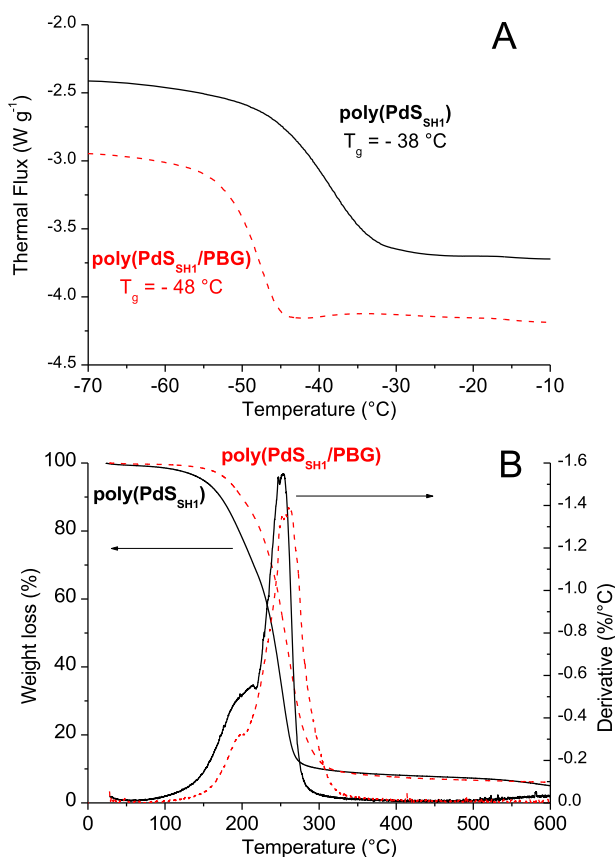
$$\frac{M(t)}{M(0)} = f_S e^{-t/T_{2S}} + f_M e^{-t/T_{2M}} + f_L e^{-t/T_{2L}}$$

where  $T_{2S}$ ,  $T_{2M}$ , and  $T_{2L}$ , respectively, represent short time (short), intermediate time (medium), and long time (long). Each relaxation is associated with a different  $T^2$  time. The relative contribution of each type of submolecules to total

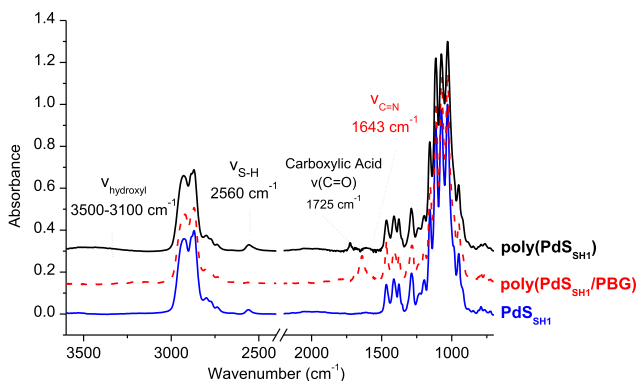
relaxation is proportional to the number of protons on these chain fragments. The three values of  $f_i$  and  $T_{2i}$  given (see inserted table in Figure 4) show that the proton relaxation of the two polymers is qualitatively different. Both poly(disulfide)s present a signal at short times ( $T_{2S}$  less than 0.5 ms), reflecting the segments whose movements are restricted and corresponding to the relaxation of a solid. Note that this signal is almost twice as high for poly(PdS<sub>SH1</sub>) ( $f_S = 31.7\%$ ) compared to poly(PdS<sub>SH1</sub>/PBG) ( $f_S = 18.2\%$ ), indicating a higher proportion of the immobilized chain. The other relaxation times  $T_{2M}$  and  $T_{2L}$  are also reduced in this system, indicative of lower mobility. In other words, the effect of UVC radiation on transverse relaxation is comparable to that of cross-linking, resulting in a greater rigidity.

**III.III. Thermal Analysis.** The DSC thermograms of poly(PdS<sub>S1</sub>) and poly(PdS<sub>SH1</sub>/PBG) are given in Figure 5A. In both samples, a negative glass-transition temperature ( $T_g$ , reflecting the formation of a more rigid structure. In both cases, TGA analysis (Figure 5B) shows two decomposition domains arising at the same temperatures of 210 and 265 °C. However, the proportion of each domain is significantly different. The structure of the poly(PdS<sub>SH1</sub>/PBG) seems relatively homogeneous as exemplified by a ratio for the two decomposition areas' ratio of 12/80 (wt %). By contrast, poly(PdS<sub>SH1</sub>) formed under UVC is more heterogeneous with a ratio of 32/62 (wt %). Its inhomogeneity is also illustrated by a degradation starting at lower temperature of 107 versus 141 °C.

**III.IV. FTIR Spectroscopy.** Figure 6 shows the FTIR spectrum of the PdS<sub>SH1</sub> oligomer and its evolution after irradiation. At 365 nm in the presence of PBG, the vibrational band  $\nu_{S-H}$  at 2560  $\text{cm}^{-1}$  was substantially decreased due to the expected SH oxidative coupling into disulfide. Note the appearance of a new vibrational band  $\nu_{C=N}$  at 1643  $\text{cm}^{-1}$  in the poly(PdS<sub>SH1</sub>/PBG) translating the TBD photogeneration. Under UVC, new vibrational modes arose in the spectrum. In agreement with solid-state NMR data, poly(PdS<sub>SH1</sub>) showed two carbonyl stretching bands at 1725  $\text{cm}^{-1}$  attributed to the carboxylic acid C=O stretch from formic esters produced by photo-oxidation of polyether chains (reaction ii, Scheme 2). The broad massif between 3100 and 3400  $\text{cm}^{-1}$  was suggestive of hydroxyl groups

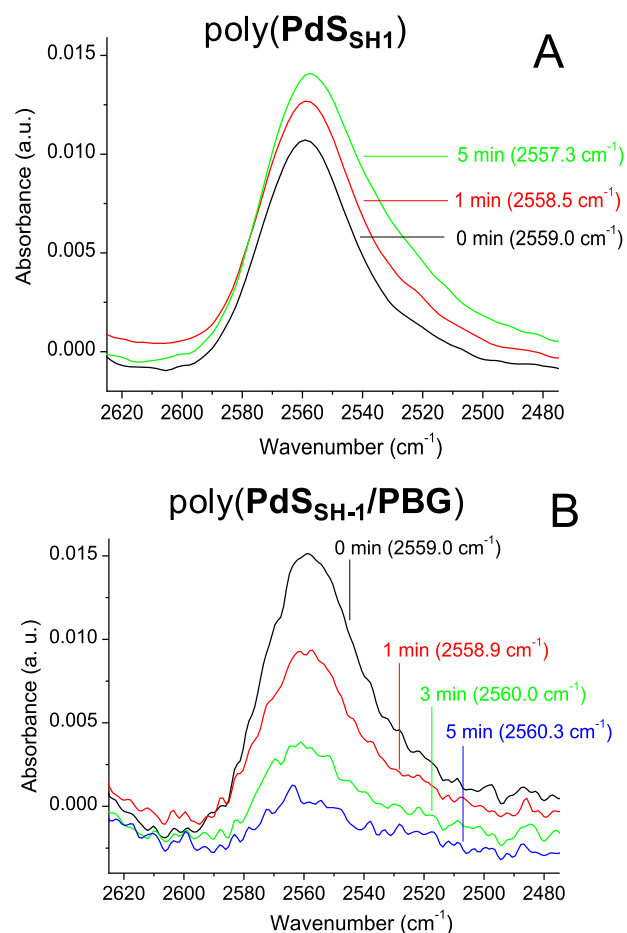


**Figure 5.** DSC (A) and TGA (B) thermograms of poly(PdS<sub>SH1</sub>) (—) and poly(PdS<sub>SH1</sub>/PBG) (- - -).



**Figure 6.** FTIR spectra of PdS<sub>SH1</sub> (—), poly(PdS<sub>SH1</sub>) (—), and poly(PdS<sub>SH1</sub>/PBG) (- - -).

and particularly alcohol groups, possibly resulting from hydrolysis (reaction iii). However, the low intensity of these vibration modes provided evidence of negligible contribution. The most striking difference between the two irradiated samples was the evolution of the  $\nu_{S-H}$  band. In poly(PdS<sub>SH1</sub>/PBG), almost complete consumption of thiol functions was observed during irradiation in accordance with the NMR data. In poly(PdS<sub>SH1</sub>), this same vibration band shows surprisingly an increase in intensity, a broadening (44% increase in area) as well as a displacement toward the lower wavenumbers ( $\Delta\bar{\nu} = -1.7 \text{ cm}^{-1}$ ) (see Figure 7). These results are contradictory to the solid-state NMR data giving approx. 90% conversion. This difference is not entirely clear and can be due to stronger interactions between SH groups in close proximity in the

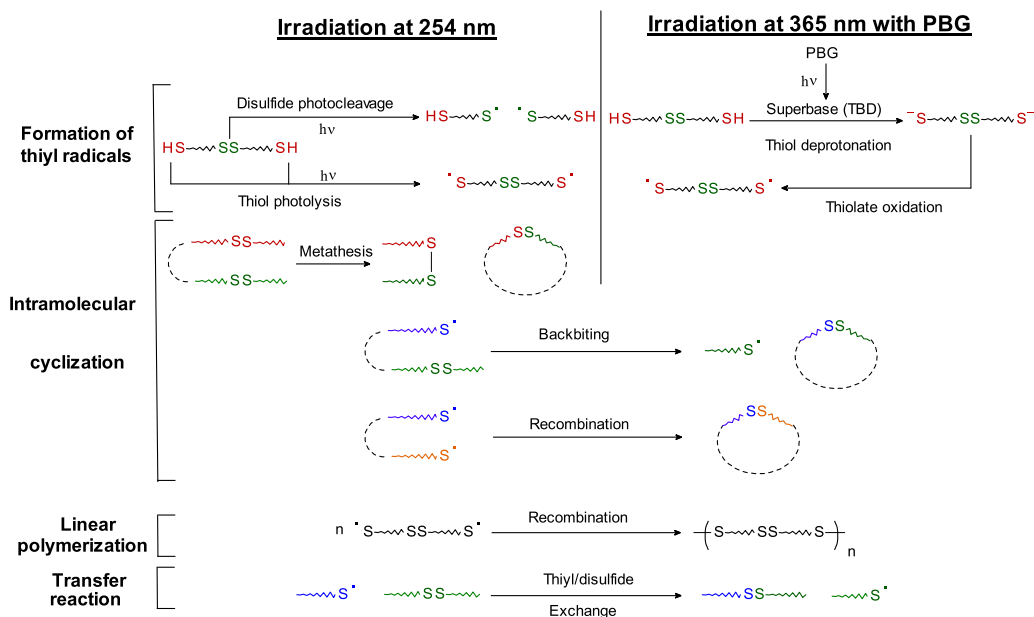
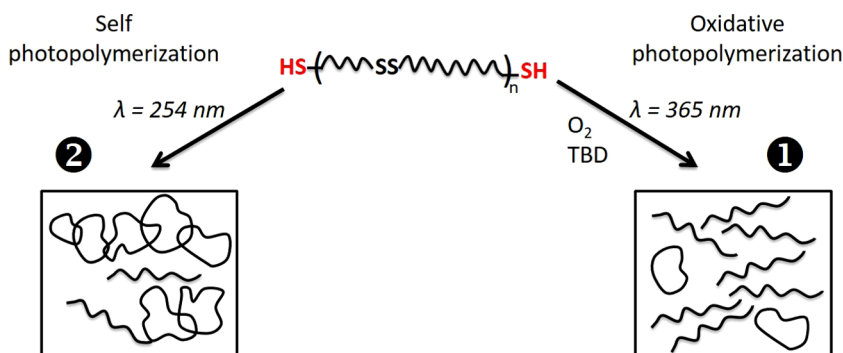


**Figure 7.** Evolution of the vibrational band  $\nu_{S-H}$  at  $2560 \text{ cm}^{-1}$  during irradiation. (A) Poly(PdS<sub>SH1</sub>) (low-pressure Hg lamp, 254 nm, 5 min). (B) Poly(PdS<sub>SH1</sub>/PBG) (LED at 365 nm, 5 min, in the presence of PBG).

poly(PdS<sub>SH1</sub>) structure. Under these conditions, a deviation in the absorption coefficient can occur, limiting the validity of the Beer–Lambert law.<sup>36</sup>

**II.III. Discussion on the Self-Photopolymerization Mechanism.** Taken together, our characterization data suggest different physicochemical properties between self-photopolymerized poly(PdS<sub>SH1</sub>) and the model poly(PdS<sub>SH1</sub>/PBG) prepared by oxidative photopolymerization. Solid-state NMR and FTIR data supported minor changes of the initial polydisulfide backbone with some limited hydrolysis and oxidation reactions of ether units (see reactions ii and iii in Scheme 2). It makes sense that photodegradation reactions are limited because of short UVC exposure times ( $\leq 8 \text{ min}$ ). In poly(PdS<sub>SH1</sub>), the main compositional change was a significant consumption of  $-SH$  terminal groups (90%). This indicates that thiol homolytic photocleavage could take place under UVC, leading to the formation of thyl radicals with the possibility of chain extension by radical coupling in a manner similar to oxidative polymerization. However, poly(PdS<sub>SH1</sub>) showed higher stiffness than poly(PdS<sub>SH1</sub>/PBG) despite a lower thiol conversion. In relaxometry, the volumetric proportion of rigid segments ( $f_s = 32\%$ ) was twice as important as in poly(PdS<sub>SH1</sub>/PBG). In addition, DSC analysis revealed a significantly higher  $T_g$  (+10 °C) and TGA data showed a more heterogeneous structure. This set of results suggests that UVC irradiation could change the polymer architecture. SS bridges' excitation might

Scheme 3. Polymerization Pathways of a PdS Resin Depending on the Irradiation Wavelength (254 or 365 nm)

Scheme 4. Competition between Intramolecular Cyclization and Linear Intermolecular Polymerization during UV Irradiation of the PdS Resin<sup>a</sup>

<sup>a</sup>At 365 nm in the presence of PBG (black circled 1), thiyl radicals result from SH deprotonation/oxidation. Distance between active centers is maximum, driving linear polymerization. At 254 nm (black circled 2), thiyl radicals result from SH and SS photolysis. Higher spatial proximity between active centers means that they are more likely to undergo direct cyclization instead of linear polymerization.

cause a rearrangement leading to a higher ratio of cyclization to linear polymerization compared with an oxidative polymerization.

To support this hypothesis, Scheme 3 describes the two photopolymerization mechanisms depending on the irradiation wavelength. First, poly(PdS<sub>SH1</sub>) and poly(PdS<sub>SH1</sub>/PBG) diverge by the generation method of thiyl radicals (RS<sup>•</sup>). In a conventional oxidative polymerization mechanism (365 nm), there is no direct excitation of the PdS resin. Photogenerated TBD (pK<sub>a</sub> ≈ 13.5) deprotonates terminal thiols to form a thiolate anion RS<sup>-</sup> acting as a much stronger nucleophile. This shift enables reaction with atmospheric oxygen to form thiyl radicals (RS<sup>•</sup>) and subsequent dimerization of the radicals to the disulfide (RS-SR). Under UVC, thiyls are generated by photocleavage of SS<sup>37,38</sup> or by photolysis of terminal HS.<sup>27</sup> After this first step, the two systems share a common step-growth polymerization mechanism where the reactive species are thiyl radicals. In any step-growth polymerization mechanism with reagents comprising two terminal groups capable of reacting with each other (A-A in our case with A = RS<sup>•</sup>),

there is competition between intramolecular cyclization and linear intermolecular polymerization. In the two cases, polysulfide macrocycles may form from backbiting or recombination reactions between 2 ends of the same chain. In the specific case of UVC irradiation, exchange reactions between disulfides (metathesis) are also possible.<sup>18,23</sup> Linear chains are formed by the coupling of thiyl radicals carried by different chains. Disulfide/thiyl exchange is also possible, leading to transfer reaction.

The probability of cycle formation depends on two antagonistic trends:<sup>39</sup> the stability of the cycle formed that increases with chain length (thermodynamic factor) and the probability of encounters between two chain ends that decreases as chain length increases (kinetic factor). On the first hand, the formation of a significant quantity of cyclic species compared to linear species has been widely reported in poly(disulfide).<sup>40</sup> The absence of termination agents and the fact that macrocycles are thermodynamically very close to linear polymers contribute to cyclization. On the other hand, the kinetic control of cyclization depends on the probability of spatial approximation between

two thiol radicals. As the potential size of the cycle increases, the speed of movement decreases, reducing the probability of encounters between thiol functions in the same chain. At 365 nm, only thiol chain ends originating from the terminal thiol can meet, which imposes a maximum distance between active centers equal to the polymer chain length (Scheme 4). Conversely, the cleavage of internal S–S bonds under UVC might favor an increase in the proportion of cyclic species because the  $RS^\bullet$  radicals are carried by smaller, more mobile and independent chains that are able to meet more easily. Consequently, the synthesis conditions under UVC could drive the kinetic control of polymerization, increasing the trend toward cyclization. In light of this reasoning, the solvent-free conditions of reaction favor the proximity between cycles and the formation of intertwining strands forming a network of mechanically entangled macrocycles. We hypothesize that the increase in the proportion of macrocycles compared to oxidative photopolymerization could be at the origin of the formation of a poly(catenane) network. This makes the poly( $PdS_{SH1}$ ) film obtained by irradiation under UVC properties comparable to cross-linked polymers. Even if this reasoning is consistent with the experimental results, we have no direct evidence of polycatenane network formation. Proof of macrocycles formation, by matrix-assisted laser desorption/ionization time-of-flight mass spectrometry for example,<sup>41</sup> was difficult to provide because of the insolubility of the sample.

### III. CONCLUSIONS

Poly(disulfide)s are resins of commercial importance in the polymer industry. Their cross-linking usually proceeds via the base-catalyzed oxidative coupling of functional thiol groups. By contrast, the bulk self-polymerization of the bifunctional oligomer film was proved to proceed under exposure to UVC irradiation (254 nm) without an oxidant and base in a few minutes only. Because the resulting film was found to be insoluble, characterization by solid-state NMR and FTIR techniques was implemented. Both techniques converged on the fact that the polydisulfide backbone was mostly preserved, displaying a chemical composition relatively similar to that of linear model polymers produced by oxidative polymerization. However, TGA, DSC, and <sup>1</sup>H relaxometry revealed different physical properties, in particular an increase of rigidity, heterogeneity, and mobility properties close to those of the cross-linked polymer. To account for these unexpected results, we postulated that UVC radiation could cause a change of the linear architecture. At 254 nm, thiol radicals are produced not only from terminal S–H bonds but also from internal SS bridges by homolytic cleavage. Because active centers are more numerous and approach each other, the rate of cyclization reaction is increased compared to linear polymerization due to kinetic control. As a result of bulk conditions, a fraction of entangled macrocycles could form, leading to cross-linking. While the proposed hypothesis was consistent with the experimental data, we were not able to prove the formation of the polycatenane network, which is generally a challenge in the literature. More research is needed to provide pieces of evidence in favor of this mechanism.

### IV. EXPERIMENTAL SECTION

**IV.I. Materials.** Used as PBG, 2-(9-oxoxanthen-2-yl)propionic acid 1,5,7-triazabicyclo [4.4.0]dec-5-ene salt was purchased from TCI. Chloroform (>99%) was supplied by

Sigma-Aldrich. Two families of difunctional liquid PdS prepolymers were supplied by AkzoNobel (Scheme 1).

- Thiol-terminated PdS with different molar masses, Thioplast G4, G21, and G10 were designated as  $PdS_{SH1}$ ,  $PdS_{SH2}$ , and  $PdS_{SH3}$ , respectively.
- Epoxy-terminated PdS, Thioplast EPS2S, was referred to as  $PdS_{Epoxy}$ .

**IV.II. Synthesis. IV.II.I. Self-Photopolymerization of PdS Oligomer ( $\lambda = 254$  nm).** A liquid  $PdS_{SH1}$  film with a thickness of 1.5  $\mu\text{m}$  was obtained by casting on a KBr pellet or glass substrate a solution containing 2 mL of chloroform and 0.48 g of  $PdS_{SH1}$  resin. Deposition was carried out by spin coating (5 s at 1000 rpm, then 10 s at 2000 rpm). The thickness value was assessed by a 3D surface profilometer. Irradiation was performed subsequently at room temperature employing two UVC irradiation sources. The first is a low-pressure Hg lamp made up of two tubes NIQ 60/35 XL (60 W, Heraeus). Placed 12 cm from the tubes, an almost monochromatic irradiation at 254 nm was received by the sample under these conditions. At this distance, the line emitted at 185 nm is almost entirely absorbed by the oxygen in the air to form ozone, and ozone is evacuated by the fume hood. The total irradiance measured at the film surface was 10.5  $\text{mW cm}^{-2}$ . A dry film was obtained after 8 min of irradiation. Alternatively, a medium-pressure Hg-Xe arc was used. It is equipped with a 254 nm reflector (Hamamatsu L8252, 200 W) to maximize the emission at 254 nm. In this case, the radiation was directed toward the sample by a waveguide placed perpendicularly 3 cm from the sample. The total irradiance measured at the film surface was 390  $\text{mW cm}^{-2}$  (200–500 nm). For inert atmosphere experiments, the samples were placed in an environmental control chamber where the temperature and atmosphere could be adjusted.

**IV.II.II. Oxidative Photopolymerization of PdS Oligomer in the Presence of PBG ( $\lambda = 365$  nm).** A typical  $PdS_{SH1}$ /PBG formulation was prepared by dissolving 20 mg of PBG in 4 mL of chloroform containing 0.48 g of  $PdS_{SH1}$  resin. This homogeneous and photolabile mixture was then deposited onto a KBr or glass substrate by spin coating (5 s at 1000 rpm and 10 s at 2000 rpm) to obtain a 1.5  $\mu\text{m}$ -thick film. The irradiation was performed by a monochromatic 365 nm LED (Phoseon Technology FJ200), which allowed obtaining a solid film after 180 s of exposure. The irradiance at 365 nm was 560  $\text{mW cm}^{-2}$ . At this emission wavelength, excitation of disulfide functions, which may cause S–S bonds' dissociation or metathesis, was prevented.

**IV.III. Methods.** UV–vis absorption spectra were acquired between 190 and 800 nm in acetonitrile with a Cary 4000 Spectrophotometer from Varian using a 10 mm quartz cuvette.

Real-time Fourier transform infrared (RT-FTIR) spectra were obtained with a Bruker Vertex 70 spectrophotometer equipped with a liquid-nitrogen-cooled mercury-cadmium-telluride (MCT) detector working in the rapid scan mode. The resolution of the spectra was 4  $\text{cm}^{-1}$  with an average of 4 scans  $\text{s}^{-1}$ . The conversion rate of thiol functions over time was determined by integration of the SH stretching band at 2570  $\text{cm}^{-1}$ . All analyses were repeated three times from samples prepared separately.

<sup>1</sup>H and <sup>13</sup>C liquid NMR (400 MHz) spectra of PdS resins were recorded at room temperature on a Bruker Avance 400 spectrometer equipped with a 5 mm Z-gradient QNP (<sup>1</sup>H, <sup>13</sup>C, <sup>19</sup>F, <sup>31</sup>P) probe for routine spectroscopy. The chemical shifts

were referenced to the residual proton signal of the solvent  $\text{CHCl}_3$  at 7.26 ppm for  $^1\text{H}$ .

Solid-state  $^1\text{H}$  MAS NMR and  $^{13}\text{C}$  MAS + DEC NMR experiments were performed at room temperature on a Bruker Avance II 400 spectrometer operating at  $B_0 = 9.4$  T (Larmor frequency  $\nu_0 = 400.17$  MHz). Single pulse experiment was recorded with a double channel 2.5 mm Bruker MAS probe, a spinning frequency of 30 kHz, a  $\pi/2$  pulse duration of 2.9  $\mu\text{s}$ , and a 5 s recycling delay.  $^1\text{H}$  spin–lattice relaxation times ( $T_1$ ) were measured with the inversion-recovery pulse sequence. Typically, 64 scans were recorded. Chemical shifts reported thereafter are relative to tetramethylsilane  $^1\text{H}$ . The deconvolution of the experimental  $^1\text{H}$  MAS spectrum was carried out with DMfit software. The conversion of thiol functions after irradiation can be calculated using deconvolutions of NMR spectra. For  $^1\text{H}$  MAS spectra, the calculation is performed by considering the signal area corresponding to the -SH protons with respect to the protons associated with the O-CH<sub>2</sub>-O function as a reference. All analyses were repeated two times from samples prepared separately.

Low field NMR  $^1\text{H}$  NMR relaxation experiments were performed in 10 mm NMR tubes on a Bruker Minispec MQ-20 spectrometer operating at proton resonance frequency of 20 MHz. The experiments were performed at 45 °C (initial magnet temperature) under static conditions. Before performing the analysis, proton spin–lattice relaxation times  $T_1$  were measured with the inversion-recovery pulse sequence

$$\pi - \tau - \frac{\pi}{2} - \tau - \text{acquisition}$$

The measurement of the time  $T_1$  allowed us to optimize and set the recycle delay in the following analyses. Next, proton spin–spin relaxation times ( $T_2$ ) were measured with different sequences and, in particular, by using the free induction decay (FID)

$$\frac{\pi}{2} - \text{acquisition}$$

and the Carr–Purcell–Meibloom–Gill (CPMG) pulse sequence (with CYCLOPS cycling)

$$\left(\frac{\pi}{2}\right)_x - (\tau - \pi_y - \tau - \text{acquisition})_n$$

where  $x$  and  $y$  are the radio-frequency phases of the pulses with angles  $\pi/2$  and  $\pi$ , respectively, and  $\tau$  is the interpulse spacing.  $\tau$  was taken at the value of 0.05 ms for all the analyses. This time is the minimal value to prevent the  $T_{1\rho}$  effect and to limit the initial intensity loss. The CPMG decay curves were deconvoluted by using a sum of exponential functions

$$M(t) = \sum_{i=1}^n A_i \exp\left(\frac{-t}{T_{2,i}}\right)$$

where  $A_i$  and  $T_{2,i}$  are, respectively, the proportion and transverse relaxation time of the proton population  $i$ . FID is the simplest NMR sequence, and its intensity is directly proportional to the total amount of protons in the sample.

Thermal gravimetric analysis (TGA) was carried out with TGA Q500 (TA Instruments) under nitrogen atmosphere (20 mL min<sup>-1</sup>). Then, 9 mg of an irradiated PdS film was placed in an open aluminum pan and heated from ambient conditions to 900 °C at 10 °C min<sup>-1</sup>.

Differential scanning calorimetry (DSC) was carried out on TA Q2000 DSC using a heat–cool–heat thermal cycle. Next, 5 mg of a poly(disulfide) film was placed in a hermetic aluminum pan. The first cycle started by heating the sample from –90 to 100 °C at 10 °C min<sup>-1</sup>. The second cycle cooled the sample back to –90 °C. The third step heated the sample again from –90 to 100 °C at 10 °C min<sup>-1</sup>.

Profilometry measurement of the liquid PdS films was carried out using a Dektak 150 (Bruker) profilometer.

## ■ ASSOCIATED CONTENT

### 📄 Supporting Information

The Supporting Information is available free of charge on the ACS Publications website at DOI: 10.1021/acsomega.9b00021.

$^{13}\text{C}$  MAS + DEC NMR spectra of poly(PdS<sub>SH1</sub>) and poly(PdS<sub>SH1</sub>/PBG) and  $^{13}\text{C}$  DEPT 135° NMR spectrum of poly(PdS<sub>SH1</sub>) in CDCl<sub>3</sub> (PDF)

## ■ AUTHOR INFORMATION

### Corresponding Author

\*E-mail: abraham.chemtob@uha.fr.

### ORCID

Abraham Chemtob: 0000-0003-4434-1870

Christian Ley: 0000-0001-7052-4692

### Notes

The authors declare no competing financial interest.

## ■ ACKNOWLEDGMENTS

The French Ministry of Higher Education and Research is acknowledged for providing a PhD scholarship to Noémi Feillée.

## ■ REFERENCES

- (1) Drobny, J. G. *Radiation Technology for Polymers*; CRC Press: Boca Raton, 2003.
- (2) Degrand, H.; Cazaux, F.; Coqueret, X.; Defoort, B.; Boursereau, F.; Larnac, G. Thermal Effects on the Network Structure of Diglycidylether of Bisphenol-A Polymerized by Electron-Beam in the Presence of an Iodonium Salt. *Radiat. Phys. Chem.* **2003**, *68*, 885–891.
- (3) Patacz, C.; Defoort, B.; Coqueret, X. Electron-Beam Initiated Polymerization of Acrylate Compositions 1: FTIR Monitoring of Incremental Irradiation. *Radiat. Phys. Chem.* **2000**, *59*, 329–337.
- (4) Cramer, N. B.; Bowman, C. N. Kinetics of Thiol–Ene and Thiol–Acrylate Photopolymerizations with Real-Time Fourier Transform Infrared. *J. Polym. Sci., Part A: Polym. Chem.* **2001**, *39*, 3311–3319.
- (5) Cramer, N. B.; Scott, J. P.; Bowman, C. N. Photopolymerizations of Thiol–Ene Polymers without Photoinitiators. *Macromolecules* **2002**, *35*, 5361–5365.
- (6) Vázquez, C. P.; Joly-Duhamel, C.; Boutevin, B. Photopolymerization without Photoinitiator of Bismaleimide-Containing Oligo-(Oxypropylene)s: Effect of Oligoethers Chain Length. *Macromol. Chem. Phys.* **2009**, *210*, 269–278.
- (7) Scherzer, T.; Knolle, W.; Naumov, S.; Elsner, C.; Buchmeiser, M. R. Self-Initiation of the UV Photopolymerization of Brominated Acrylates. *J. Polym. Sci., Part A: Polym. Chem.* **2008**, *46*, 4905–4916.
- (8) Scherzer, T. VUV-Induced Photopolymerization of Acrylates. *Macromol. Chem. Phys.* **2012**, *213*, 324–334.
- (9) Wang, H.; Brown, H. R. Self-Initiated Photopolymerization and Photografting of Acrylic Monomers. *Macromol. Rapid Commun.* **2004**, *25*, 1095–1099.
- (10) Vietti, D.; Scherrer, M. Polymers Containing Sulfur, Polysulfides. In *Kirk-Othmer Encyclopedia of Chemical Technology*; John Wiley & Sons, 2000.

- (11) Khakimullin, Y. N.; Minkin, Y. N.; Deberdeev, T. R.; Zaikov, G. E. *Polysulfide Oligomer Sealants: Synthesis, Properties and Applications*; CRC Press: Boca Raton, 2015.
- (12) Niu, Z.; Gibson, H. W. Polycatenanes. *Chem. Rev.* **2009**, *109*, 6024–6046.
- (13) Blanco, M.-J.; Jiménez, M. C.; Chambron, J.-C.; Heitz, V.; Linke, M.; Sauvage, J.-P. Rotaxanes as New Architectures for Photoinduced Electron Transfer and Molecular Motions. *Chem. Soc. Rev.* **1999**, *28*, 293–305.
- (14) Endo, K.; Shiroy, T.; Murata, N.; Kojima, G.; Yamanaka, T. Synthesis and Characterization of Poly(1,2-Dithiane). *Macromolecules* **2004**, *37*, 3143–3150.
- (15) Endo, K.; Yamanaka, T. Copolymerization of Lipoic Acid with 1,2-Dithiane and Characterization of the Copolymer as an Interlocked Cyclic Polymer. *Macromolecules* **2006**, *39*, 4038–4043.
- (16) Yamanaka, T.; Endo, K. Network Formation of Interlocked Copolymer Obtained from Copolymerization of 1,2-Dithiane and Lipoic Acid by Metal Salt. *Polym. J.* **2007**, *39*, 1360–1364.
- (17) Bookwalter, C.; Zoller, D.; Ross, P.; Johnston, M. Bond-Selective Photodissociation of Aliphatic Disulfides. *J. Am. Soc. Mass Spectrom.* **1995**, *6*, 872–876.
- (18) Otsuka, H.; Nagano, S.; Kobashi, Y.; Maeda, T.; Takahara, A. A Dynamic Covalent Polymer Driven by Disulfide Metathesis under Photoirradiation. *Chem. Commun.* **2010**, *46*, 1150–1152.
- (19) Canadell, J.; Goossens, H.; Klumperman, B. Self-Healing Materials Based on Disulfide Links. *Macromolecules* **2011**, *44*, 2536–2541.
- (20) Michal, B. T.; Jaye, C. A.; Spencer, E. J.; Rowan, S. J. Inherently Photohealable and Thermal Shape-Memory Polydisulfide Networks. *ACS Macro Lett.* **2013**, *2*, 694–699.
- (21) Gao, W.; Bie, M.; Liu, F.; Chang, P.; Quan, Y. Self-Healable and Reprocessable Polysulfide Sealants Prepared from Liquid Polysulfide Oligomer and Epoxy Resin. *ACS Appl. Mater. Interfaces* **2017**, *9*, 15798–15808.
- (22) An, S. Y.; Noh, S. M.; Nam, J. H.; Oh, J. K. Dual Sulfide–Disulfide Crosslinked Networks with Rapid and Room Temperature Self-Healability. *Macromol. Rapid Commun.* **2015**, *36*, 1255–1260.
- (23) Ohishi, T.; Iki, Y.; Imato, K.; Higaki, Y.; Takahara, A.; Otsuka, H. Insertion Metathesis Depolymerization of Aromatic Disulfide-Containing Dynamic Covalent Polymers under Weak Intensity Photoirradiation. *Chem. Lett.* **2013**, *42*, 1346–1348.
- (24) Chemtob, A.; Feillée, N.; Ley, C.; Ponche, A.; Rigolet, S.; Soraru, C.; Ploux, L.; Le Nouen, D. Oxidative Photopolymerization of Thiol-Terminated Polysulfide Resins. Application in Antibacterial Coatings. *Prog. Org. Coat.* **2018**, *121*, 80–88.
- (25) Feillée, N.; De Fina, M.; Ponche, A.; Vaulot, C.; Rigolet, S.; Jacomine, L.; Majjad, H.; Ley, C.; Chemtob, A. Step-Growth Thiol–Thiol Photopolymerization as Radiation Curing Technology. *J. Polym. Sci., Part A: Polym. Chem.* **2017**, *55*, 117–128.
- (26) Koji, A.; Endo, R. Application to Photoreactive Materials of Photochemical Generation of Superbases with High Efficiency Based on Photodecarboxylation Reactions. *Chem. Mater.* **2013**, *22*, 4461–4463.
- (27) Knight, A. R. Photochemistry of Thiols. In *The Thiol Group*; John Wiley & Sons, 1974; pp 455–479.
- (28) Sheraton, D. F.; Murray, F. E. Quantum Yields in the Photolytic Oxidation of Some Sulphur Compounds. *Can. J. Chem.* **1981**, *59*, 2750–2754.
- (29) Lee, Y. R.; Chiu, C. L.; Lin, S. M. Ultraviolet Photodissociation Study of CH<sub>3</sub>SCH<sub>3</sub> and CH<sub>3</sub>SSCH<sub>3</sub>. *J. Chem. Phys.* **1994**, *100*, 7376–7384.
- (30) Freeman, F.; Angeletakis, C. N.; Maricich, T. J. <sup>1</sup>H NMR and <sup>13</sup>C NMR Spectra of Disulfides, Thiosulfonates and Thiosulfonates. *Org. Magn. Reson.* **1981**, *17*, 53–58.
- (31) Robert-Banchereau, E.; Lacombe, S.; Ollivier, J. Unsensitized Photooxidation of Sulfur Compounds with Molecular Oxygen in Solution. *Tetrahedron* **1997**, *53*, 2087–2102.
- (32) Morlat, S.; Gardette, J.-L. Phototransformation of Water-Soluble Polymers. I: Photo- and Thermooxidation of Poly(Ethylene Oxide) in Solid State. *Polymer* **2001**, *42*, 6071–6079.
- (33) Mahon, A.; Kemp, T. J.; Coates, R. J. Thermal and Photodegradation of Polysulfide Pre-Polymers: Products and Pathways. *Polym. Degrad. Stab.* **1998**, *62*, 15–24.
- (34) Caddy, M.; Kemp, T. J. Photoactive Liquid Polysulfides: Preparation, Characterisation, Photocuring and Potential Applications. *Eur. Polym. J.* **2003**, *39*, 461–487.
- (35) Litvinov, V. M.; Dias, A. A. Analysis of Network Structure of UV-Cured Acrylates by H-1 NMR Relaxation, C-13 NMR Spectroscopy, and Dynamic Mechanical Experiments. *Macromolecules* **2001**, *34*, 4051–4060.
- (36) Davidson, R. G.; Mathys, G. I. The Determination of Thiol Groups in Polysulfide Prepolymers by Infrared Spectrometry. *Anal. Chim. Acta* **1984**, *160*, 197–204.
- (37) Oae, S. *Organic Sulfur Chemistry: Structure and Mechanism*; CRC Press: Boca Raton, 1991.
- (38) Banchereau, E.; Lacombe, S.; Ollivier, J. Solution Reactivity of Thiol Radicals with Molecular Oxygen: Unsensitized Photooxidation of Dimethyldisulfide. *Tetrahedron Lett.* **1995**, *36*, 8197–8200.
- (39) Mercier, J. P.; Maréchal, E. *Chimie Des Polymères - Synthèses, Réactions, Dégradations*; Traité des Matériaux; Presses polytechniques et universitaires romandes: Lausanne, Suisse, 1996; Vol. 13.
- (40) Endo, K. Synthesis and Properties of Cyclic Polymers. In *New Frontiers in Polymer Synthesis*; Kobayashi, S., Ed.; Advances in Polymer Science; Springer: Berlin, 2008; pp 121–183.
- (41) Rosenthal, E. Q.; Puskas, J. E.; Wesdemiotis, C. Green Polymer Chemistry: Living Dithiol Polymerization via Cyclic Intermediates. *Biomacromolecules* **2012**, *13*, 154–164.